J. Biochem. **141**, 85–91 (2007)
doi:10.1093/jb/mvm010

Membrane Topology of Aspartate:Alanine Antiporter AspT from *Comamonas testosteroni*

Takashi Fujiki[1], Kei Nanatani[1], Kei Nishitani[1], Kyoko Yagi[1], Fumito Ohnishi[1], Hiroshi Yoneyama[2], Takafumi Uchida[1], Tasuku Nakajima[1] and Keietsu Abea[1,*]

[1]Laboratory of Enzymology; and [2]Laboratory of Dairy Microbiology, Department of Molecular and Cell Biology, Graduate School of Agricultural Science, Tohoku University, Sendai, 981-8555 Japan

Received October 17, 2006; accepted November 15, 2006; published online December 11, 2006

We cloned the *aspT* gene encoding the L-aspartate:L-alanine antiporter $AspT_{Ct}$ in *Comamonas testosteroni* genomic DNA. Analysis of the nucleotide sequence revealed that *C. testosteroni* has an *asp* operon containing *aspT* upstream of the L-aspartate 4-decarboxylase gene, and that the gene order of the *asp* operon of *C. testosteroni* is the inverse of that of *Tetragenococcus halophilus*. We used proteoliposomes to confirm the transport processes of $AspT_{Ct}$. To elucidate the two-dimensional structure of $AspT_{Ct}$, we analysed its membrane topology by means of alkaline phosphatase (PhoA) and β-lactamase (BlaM) fusion methods. The fusion analyses revealed that $AspT_{Ct}$ has seven transmembrane segments (TMs), a large cytoplasmic loop containing ~200 amino acid residues between TM4 and TM5, a cytoplasmic N-terminus, and a periplasmic C-terminus. These results suggest that the orientation of the N-terminus of $AspT_{Ct}$ differs from that of tetragenococcal AspT, even though these two AspT orthologues catalyse the same transport reactions.

Key words: aspartate:alanine antiporter, bacteria, bioenergetics, fusion methods, membrane topology.

INTRODUCTION

Comamonas testosteroni (previously called *Pseudomonas dacunhae*) is a Gram-negative bacterium. This bacterium is used as an immobilized biocatalyst for the industrial production of L-alanine and L-aspartate because its L-aspartate 4-decarboxylase (AspD) possesses high specific activity. AspDs are found in several bacteria, and the enzymology of these proteins has been studied. Since Mardashev and Gladkova (*1*) discovered AspD in *Pseudomonas mycobacterium* (*1*), AspDs have been found in *Clostridium perfringens* (*2, 3*), *Desulfovibrio desulfurican* (*4, 5*), *Nocardia globerula* (*6*), a strain of *Acetobacter* (*7*), *Achromobacter* d-15 (*8, 9*), and *Alcaligenes faecalis* (*10, 11*). Chibata *et al*. also found several bacterial AspDs with high specific activities; AspD from *C. testosteroni* showed the highest specific activity (*12*).

We previously reported that some strains of a *Lactobacillus* subsp. (*13*) and the halophilic lactic acid bacterium *Tetragenococcus halophilus* (previously called *Pediococcus halophilus*) catalyse the decarboxylation of L-aspartate with near-stoichiometric release of L-alanine and CO_2. L-aspartate decarboxylation is thought to be advantageous to bacterial cells, because L-aspartate consumption concomitant with the release of L-alanine generates, rather than consumes, metabolic energy and regulates intracellular pH (*14*). In these two Gram-positive bacteria, we further identified antiporter AspTs that catalyse an electrogenic exchange reaction of L-aspartate with L-alanine (*13, 14*). The net charge movement during the exchange reaction results in a membrane potential of physiological polarity. Furthermore, decarboxylation reactions consume scalar protons and thus generate a pH gradient of physiological polarity. In one strain, *T. halophilus* D10, Abe *et al*. found a 25-kb plasmid responsible for the trait of L-aspartate decarboxylation; they cloned and sequenced the *asp* operon, which consists of two genes designated $aspD_{Th}$ and $aspT_{Th}$. $aspD_{Th}$ encodes an L-aspartate 4-decarboxylase ($AspD_{Th}$), and $aspT_{Th}$ an aspartate:alanine antiporter ($AspT_{Th}$) (*14*). Nanatani *et al*. analysed the membrane topology of $AspT_{Th}$ by using alkaline phosphatase (PhoA) and β-lactamase (BlaM) fusion methods (*15*). $AspT_{Th}$ possesses a unique structure with extracellular N- and C-termini, eight transmembrane segments (TMs), and one large cytoplasmic loop. This protein originally served to characterize the aspartate:alanine exchanger (AAE) family of secondary transporters (Saier *et al*., http://www.tcdb.org/).

Because *C. testosteroni* is among the industrial microorganisms with the highest conversion efficiency with respect to L-aspartate decarboxylation, we predicted that AspT was present in *C. testosteroni* ($AspT_{Ct}$). The aim of this study was to determine whether the structure and function of $AspT_{Ct}$ differed from those of $AspT_{Th}$, the membrane topology and transport processes of which have been biochemically characterized. We found that an *asp* operon was present in *C. testosteroni* genome and that the gene order of the operon ($aspT_{Ct} \rightarrow aspD_{Ct}$) was the inverse of that of the *T. halophilus asp* operon ($aspD_{Th} \rightarrow aspT_{Th}$). We cloned $aspT_{Ct}$ and compared

*To whom correspondence should be addressed. Tel: +81-22-717-8777, Fax: +81-22-717-8778, E-mail: kabe@biochem.tohoku.ac.jp

the membrane topology of $AspT_{Ct}$ with that of $AspT_{Th}$ by fusion methods. The differences between the two-dimensional structures of the two AspTs are discussed.

MATERIALS AND METHODS

Bacterial Strains and Plasmids—Comamonas testosteroni (previously called *P. dacunhae* ATCC 21192) was the source of genomic DNA for the cloning of $aspD_{Ct}$ and $aspT_{Ct}$ genes encoding L-aspartate 4-decarboxylase (*16*) and aspartate:alanine antiporter, respectively. The strains of *Escherichia coli* used in this work have been described previously (*14, 15*).

Hydropathy Analysis of $AspT_{Ct}$—The hydropathy profile of $AspT_{Ct}$ was derived by the method of Eisenberg *et al*.(*17*) using a sliding window of 15 amino acids (AA).

Analysis of $AspT_{Ct}$–PhoA and $AspT_{Ct}$–BlaM Fusion Proteins—We biochemically investigated the two-dimensional membrane topology of $AspT_{Ct}$ by using PhoA and BlaM fusion methods, as described previously (*15*). Deletion derivatives of $AspT_{Ct}$ were amplified from plasmid pUC 119 including the $aspT_{Ct}$ gene by PCR using primers that generated unique restriction sites at the 5′ (*Spe* I) and 31′ (*Kpn* I) ends. *Spe* I sites were introduced 2-bp downstream of each *Nco* I site of pBAD*phoA* and pYZ4 or 3-bp downstream of the *Nde* I site of pET-39b (+), by means of site-directed mutagenesis. The 3′ sites were designed to create in-frame fusions to the reporter cassettes upon ligation into either pBAD*phoA* (PhoA), pYZ4 (BlaM), or pET-39b (+) (BlaM). The plasmid pYZ4 was used for expression of most fusions, except for BlaM fusions at the N-terminus of $AspT_{Ct}$ and some BlaM fusions at the truncated C-termini of $AspT_{Ct}$, because the exceptions were not expressed by pYZ4. Instead of pYZ4, pET-39b (+) was used for expression of the exceptions. The production of fusion proteins derived from pYZ–$aspT_{Ct}$–*blaM* is under the control of the *lacUV5* promoter. pET–*blaM*–$aspT_{Ct}$ and pET–$aspT_{Ct}$–*blaM* are under the control of the T7*lac* promoter, and the downstream gene of the T7*lac* promoter is transcribed by T7 RNA polymerase. This transcription is under the control of the *lacUV5* promoter of the host cell, BL21 (DE3), therefore, production of the fusion proteins was induced in the presence of isopropyl β-D-thiogalactoside (IPTG). Fusions derived from pYZ–$aspT_{Ct}$–*blaM* or pET–*blaM*–$aspT_{Ct}$ were induced by shaking with IPTG at 1 mM or 50 μM, respectively, for 2 h at 27°C. The fusion constructs were sequenced to verify the fusion junctions. Alkaline phosphatase-specific activities of the $AspT_{Ct}$–PhoA chimeras were determined as described by Guan *et al*. (*18*). *E. coli* (strain LMG194) bearing fusion constructs were grown to $A_{650} = 0.5$. Cultures were then induced to make *E. coli* strains produce the fusion proteins in the presence of 0.4% L-arabinose. The cells that produced the fusion proteins were treated with sodium dodecyl sulphate (SDS) and chloroform; then alkaline phosphatase activities were measured.

The minimal inhibitory concentrations (MICs) of carbenicillin for strains expressing $AspT_{Ct}$–BlaM fusions were determined by spotting 5 μl of a 10^{-3} dilution of a suspension culture containing cells grown to $A_{650} = 0.5$ onto Luria–Bertani (LB) agar plates containing the antibiotics. In the case of the pET expression system, 25 μM IPTG was added to each LB agar plate. The plates were incubated at 30°C for 24 h (in the case of XL3) or 16 h (in the case of BL21 (DE3). The concentrations of carbenicillin ranged from 0 to 800 μg/ml.

Preparation of Membrane Fraction Proteins—Membrane fractions were prepared for Western blot analysis of the fusion proteins. Each *E. coli* strain bearing fusion constructs and the plasmid without fusion was grown to $A_{650} = 0.5$. Cultures were then induced to make *E. coli* strains produce the fusion proteins. After induction, the cells were harvested by centrifugation at 2190*g* for 15 min at 4°C. Then the cell pellets were washed with phosphate-buffered saline (PBS) (137 mM NaCl, 8.1 mM Na_2HPO_4, 2.68 mM KCl, 1.47 mM KH_2PO_4 (pH 7.4)), and pellets resuspended with 500 μl PBS were disrupted by sonication using a Bioruptor UCD-130T (COSMO BIO, Tokyo, Japan). The disrupted cells were treated by ultracentrifugation at 120000*g* for 60 min at 4°C. Then the supernatant was discarded, and the pellets of membrane vesicles were suspended in PBS of the 50–100 μl. The quantity of the protein contained in the membrane vesicles was determined as described by Schaffner and Weissmann (*19*).

SDS–PAGE and Western Blotting—The membrane vesicles containing the fusion proteins were suspended at a concentration of 1 or 2 μg protein/μl in loading buffer [0.12 M Tris-HCl (pH 8.8), 10% glycerol, 5% SDS, 5% 2-mercaptoethanol, 0.05% bromophenol blue] and incubated for 1 h at 37°C, after which time 15 μl samples were loaded onto SDS–polyacrylamide gels containing 10 or 12.5% polyacrylamide. After electrophoresis, the proteins were transferred to a polyvinylidene difluoride (PVDF) membrane (Nippon Genetics, Tokyo, Japan) by semidry electrophoretic blotting, and visualized by immunoblotting using antibacterial alkaline phosphatase mouse monoclonal antibodies or anti- β-lactamase mouse polyclonal antibodies (*15*).

Nucleotide Sequence Accession Number—The nucleotide sequence of the *C. testosteroni* (*P. dacunhae*) *asp* operon ($aspT_{ct}$, $aspD_{ct}$) has been deposited in the DDBJ/EMBL/GenBank nucleotide sequence database under accession number AB091385.

Other Methods—Methods for cloning of the *C. testosteroni asp* operon, expression of the *C. testosteroni asp* operon in *E. coli*, preparation of membrane vesicles, solubilization, reconstitution of $AspT_{Ct}$, and assay of aspartate transport are provided in the online Supplementary Information.

RESULTS AND DISCUSSION

Cloning of the C. testosteroni Asp Operon—$aspT_{Th}$ is the only known gene encoding an aspartate:alanine antiporter for which an electrogenic aspartate:alanine exchange reaction has been biochemically demonstrated (*14*). Although some strains of *C. testosteroni*

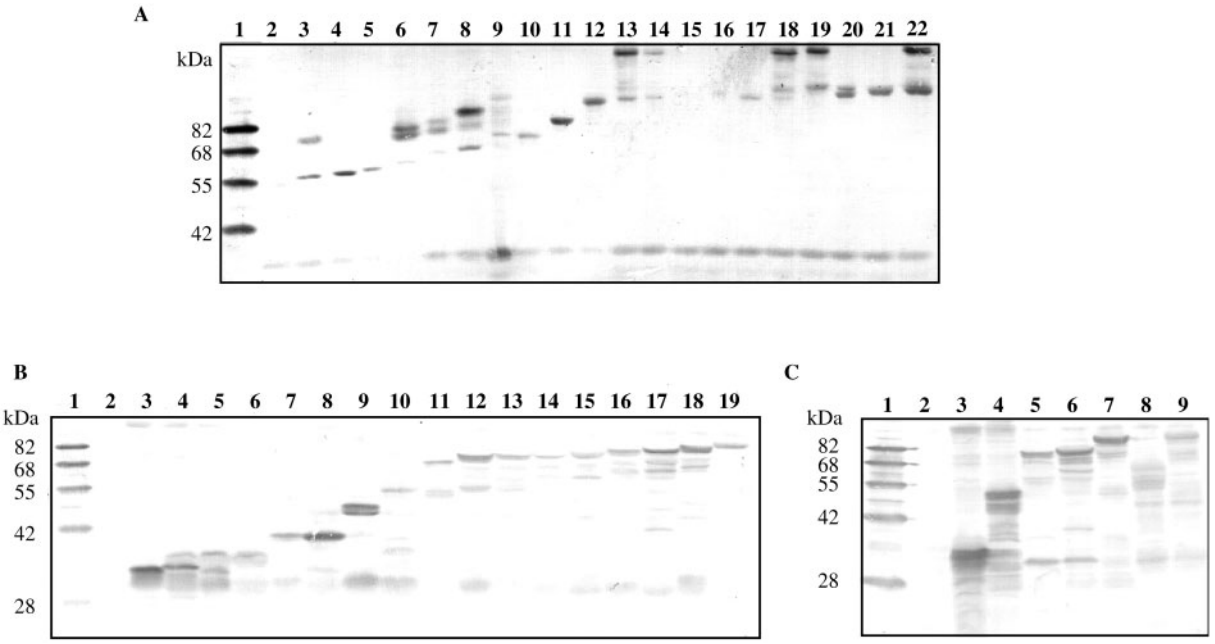

Fig. 1. **Western blot analysis of AspT$_{Ct}$–PhoA fusion proteins produced in *E. coli* LMG194 (A), AspT$_{Ct}$–BlaM fusion proteins produced in *E. coli* XL-3 (B), and AspT$_{Ct}$–BlaM fusion proteins produced in *E. coli* BL21 (DE3) (C).** Membrane fractions were prepared, subjected to electrophoresis on SDS–polyacrylamide gels containing 10% polyacrylamide, electroblotted onto a polyvinylidene difluoride membrane, and visualized with monoclonal antibodies against alkaline phosphatase (A) or polyclonal antibodies against β-lactamase (B, C). The samples are coded here according to the fusion site (e.g., Gly^{23} indicates residues 1–23 of native AspT fused with PhoA). (A) Lane 1, molecular weight markers (Western doctor); lane 2, vector (pBAD*phoA*); lane 3, C-Gly^{23}; lane 4, C-Leu^{36}; lane 5, C-Leu^{44}; lane 6, C-Lys^{61}; lane 7, C-Ser^{88}; lane 8, C-Leu^{115}; lane 9, C-Glu^{142}; lane 10, C-Arg^{190}; lane 11, C-Val^{258}; lane 12, C-Lys^{383}; lane 13, C-Ser^{422}; lane 14, C-Trp^{428}; lane 15, C-Lys^{433}; lane 16, C-Leu^{446}; lane 17, C-Ala^{453}; lane 18, C-Gln^{462}; lane 19, C-Thr^{477}; lane 20, C-Arg^{502}; lane 21, C-Lys^{529}; and lane 22, C-Ala^{561}. (B) Lane 1, molecular weight markers (Western doctor); Lane 2, vector (pYZ4); lane 3, C-Gly^{23}; lane 4, C-Leu^{36}; lane 5, C-Leu^{44}; lane 6, C-Lys^{61}; lane 7, C-Ser^{88}; lane 8, C-Leu^{115}; lane 9, C-Glu^{142}; lane 10, C-Val^{258}; lane 11, C-Lys^{383}; lane 12, C-Ser^{422}; lane 13, C-Lys^{433}; lane 14, C-Leu^{446}; lane 15, C-Gln^{462}; lane 16, C-Thr^{477}; lane 17, C-Arg^{502}; lane 18, C-Lys^{529}; and lane 19, C-Ala^{561}. (C) Lane 1, molecular weight markers (Western doctor); lane 2, vector (pET39b); lane 3, C-Gly^{23}; lane 4, C-Ala^{196}; lane 5, C-Trp^{428}; lane 6, C-Ala^{453}; lane 7, C-Ala^{561}; lane 8, N-AspT$_{Ct}$ (half-length); and lane 9, N-AspT$_{Ct}$ (full-length).

show high activity for L-aspartate decarboxylation and have thus been used for industrial production of L-alanine, the transport processes of aspartate and alanine remain unclear in *C. testosteroni*. The *C. testosteroni aspD* gene (*aspD*$_{Ct}$) was isolated by Rozzell (*20*). We carefully searched the 5′ upstream and 3′ downstream regions of *aspD*$_{Ct}$ and found part of an open reading frame (ORF) encoding a membrane protein immediately upstream of the 5′ end of *aspD*$_{Ct}$. Thus, we screened a genomic DNA library of *C. testosteroni* by colony hybridization using *aspD*$_{Ct}$ as a hybridization probe, and we isolated positive clones in which each plasmid had a 5.6-kb *Eco*R I and *Hin*d III fragment. Determination of the nucleotide sequence of the insert revealed that a gene encoding a putative membrane protein having multiple TMs was located 47-bp immediately upstream of the 5′ end of *aspD*$_{Ct}$ and that this gene, along with *aspD*$_{Ct}$, probably organized the *asp* operon of *C. testosteroni* (Supplementary Figure 1A). We designated the gene encoding this membrane protein *aspT*$_{Ct}$. There was no potential ORF immediately upstream of the 5′ end of *aspT*$_{Ct}$ or downstream of the 3′ end of *aspD*$_{Ct}$ in this direction; the minimum size for a putative ORF used to analyse the sequence was 40 A.A. The organization of the *C. testosteroni asp* operon (*aspT*$_{Ct}$ → *aspD*$_{Ct}$) was the inverse of that of the *T. halophilus asp* operon (*aspD*$_{Th}$ → *aspT*$_{Th}$) (Supplementary Figure 1B).

Expression of the Asp Operon of C. testosteroni in E. coli—To determine whether the gene tentatively identified as *aspT*$_{Ct}$ encoded the AspT$_{Ct}$ transport protein, we constructed a vector (pTrc-*asp*$_{Ct}$) that brought protein production under the control of the *trc* promoter. Production of the encoded protein and assays of its function were then carried out in *E. coli* XL3. The *E. coli* cells harboring pTrc-*asp*$_{Ct}$ expressed AspD$_{Ct}$ and AspT$_{Ct}$ in the presence of IPTG. The experiments described in Supplementary Figure 2 revealed that the gene identified as *aspT*$_{Ct}$ encodes the AspT$_{Ct}$ transport protein and that the main features of AspT$_{Ct}$ function are retained in *E. coli*.

Reconstitution of AspT$_{Ct}$ in Proteoliposomes—We initially focused on studying aspartate-loaded proteoliposomes, with the expectation that AspT$_{Ct}$ would catalyse an aspartate self-exchange. The steady-state incorporation of (^{3}H)aspartate was approximately 13.9 nmol/mg of protein (Supplementary Figure 2A). Moreover, the incorporated material was readily expelled by the later addition of excess unlabeled aspartate or alanine,

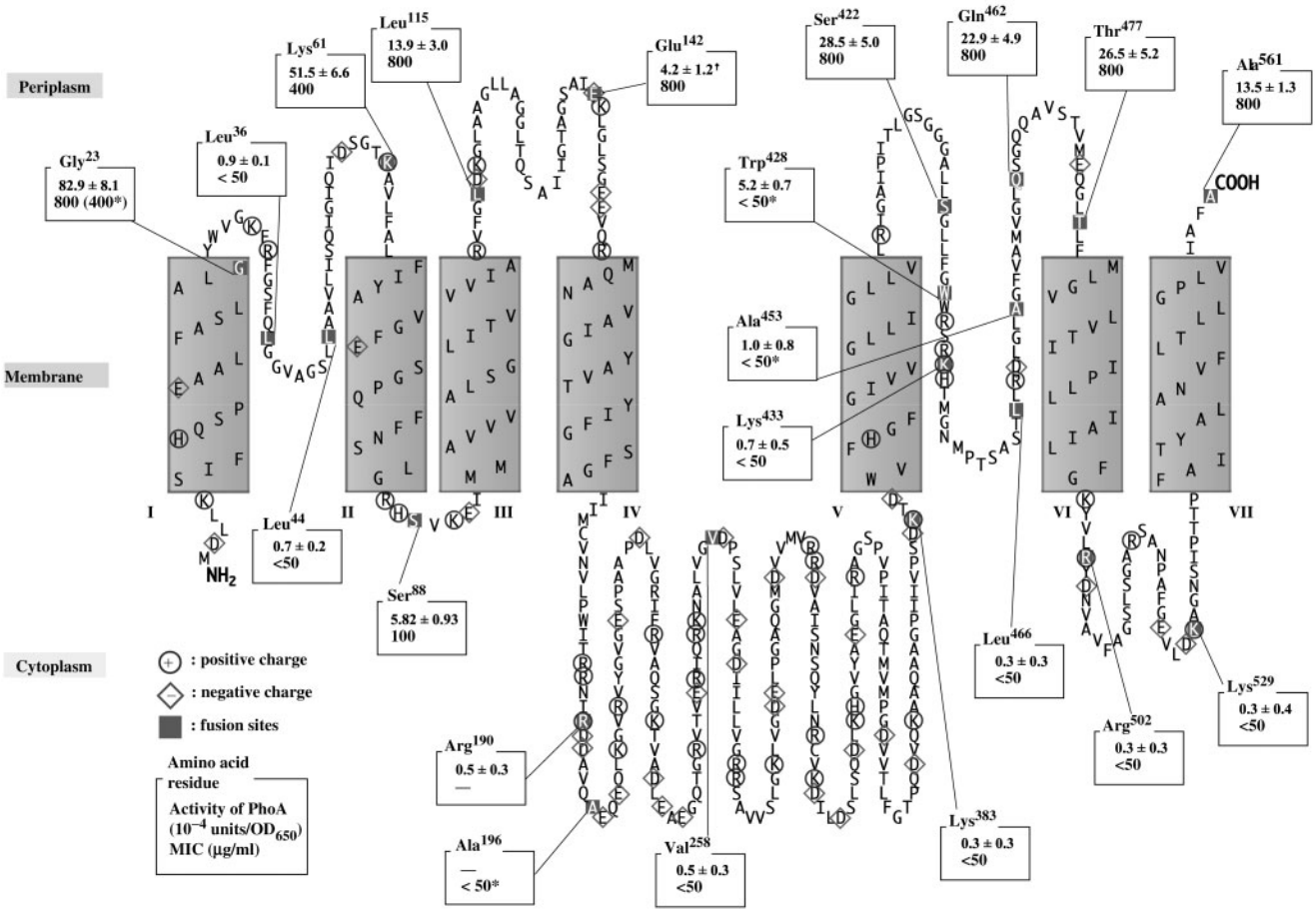

Fig. 2. **Topological model of $AspT_{Ct}$, based on the results of PhoA fusions and BlaM fusions**.

suggesting that (^{3}H)aspartate was taken up by a self-exchange reaction with aspartate and that alanine was the counter-substrate for aspartate. Since accumulated (^{3}H)aspartate was released by addition of either aspartate or alanine (Supplementary Figure 2B), it seems feasible that both compounds served as substrates for $AspT_{Ct}$.

Hydropathy Analyses of $AspT_{Ct}$—A hydropathy profile of $AspT_{Ct}$ was derived by the method of Eisenberg (*17*) using a sliding window of 15 A.A. Although the amino acid sequence alignment showed that the residues of $AspT_{Ct}$ were 27.7% identical to those of $AspT_{Th}$, the hydropathy profile of $AspT_{Ct}$ is similar to that of $AspT_{Th}$. Both $AspT_{Ct}$ and $AspT_{Th}$ have a large hydrophilic central loop encompassed by hydrophobic segments in their N- and C-terminal halves (*15*). Further analyses of $AspT_{Ct}$ hydropathy by using the programs SOSUI [http://sosui.proteome.bio.tuat.ac.jp/sosuiframe0.html (*21*)], TMHMM [http://www.cbs.dtu.dk/services/TMHMM/ (*22, 23*)], and TMPred [http://www.ch.embnet.org/software/TMPRED_form.html (*24*)] predicted the presence of eight or nine TMs in $AspT_{Ct}$. Because of the discrepancies of the results from the three computational prediction methods, the number of TMs is unclear.

Analysis of $AspT_{Ct}$–PhoA Fusion Proteins—We biochemically investigated the two-dimensional membrane topology of $AspT_{Ct}$ by using PhoA and BlaM fusion methods. The locations of these fusions, along with their enzymatic activities and subcellular locations, are given in Table 1. Production of the fusion proteins was confirmed by Western blot analyses with antibodies against PhoA or BlaM (Fig. 1). The mobility of most of the fusion proteins was within a range appropriate to their expected molecular masses. Production levels of the fusion protein with junction sites located after Lys^{433} of $AspT_{Ct}$ were too low for detection of the band, but we could confirm its expression by loading a larger amount of proteins (30 μg) onto SDS–polyacrylamide gels (data not shown). Fusion proteins with junction sites located after Gly^{23}, Lys^{61}, Leu^{115}, Ser^{422}, Gln^{462}, Thr^{477}, and Ala^{561} of $AspT_{Ct}$ showed high alkaline phosphatase activity ($>10 \times 10^{-4}$ units/OD_{650}), indicating localization of these sites at, or close to, the periplasmic side of the membrane. The alkaline phosphatase activity of the $AspT_{Ct}$–PhoA fusion construct at Glu^{142} was lower than 10×10^{-4} units/OD_{650}. However, the $AspT_{Ct}$–PhoA fusion at Thr^{136} showed $14.8 \pm 2.4 \times 10^{-4}$ units/OD_{650} (data not shown). In addition, the results of $AspT_{Ct}$–BlaM fusion analysis described subsequently suggest that the segment around Thr^{136} and Glu^{142} faced, or was close to, the periplasmic side. The low activity of the fusion site at Glu^{142} might have been caused by disorder of the PhoA segment at the specific locus. Low alkaline phosphatase

Table 1. **Characteristics of AspT$_{Ct}$ chimeric proteins.**

Amino acid residue of fusion position[a]	Activity of PhoA (10^{-4} units/OD 650)[b]	MIC (μg/ml)[c] of carbenicillin	Localization[d]
N-AspT (full-length)[e]		<50*	In
N-AspT (half)		<50*	In
Gly^{23}	82.9 ± 8.1	800 (400*)	Out
Leu^{36}	0.9 ± 0.1	<50	M
Leu^{44}	0.7 ± 0.2	<50	M
Lys^{61}	51.5 ± 6.6	400	Out
Ser^{88}	5.82 ± 0.93	100	In
Leu^{115}	13.9 ± 3.0	800	Out
Glu^{142}	4.2 ± 1.2†	800	Out
Arg^{190}	0.5 ± 0.3	No Data	In
Ala^{196}	No Data	<50*	In
Val^{258}	0.5 ± 0.3	<50*	In
Lys^{383}	0.3 ± 0.3	<50*	In
Ser^{422}	28.5 ± 5.0	800	Out
Trp^{428}	5.2 ± 0.7	<50*	M
Lys^{433}	0.7 ± 0.5	<50	M
Leu^{446}	0.3 ± 0.3	<50	M
Ala^{453}	1.0 ± 0.8	<50*	M
Gln^{462}	22.9 ± 4.9	800	Out
Thr^{477}	26.5 ± 5.2	800	Out
Arg^{502}	0.3 ± 0.3	<50	In
Lys^{529}	0.3 ± 0.4	<50	In
Ala^{561}	13.5 ± 1.3	800 (400*)	Out

[a]Last amino acid residue of original AspT$_{Ct}$ before the fusion point. [b]Alkaline phosphatase activity was measured in exponentially growing suspension cultures. [c]Carbenicillin resistance of *E. coli* XL3, or BL21(DE3) cells producing AspT$_{Ct}$ BlaM fusion proteins was measured as the single-cell minimum inhibitory concentration (MIC). *Means *E. coli* BL21(DE3) strain was used in the assay. [d]Location as determined by alkaline phosphatase specific activity and the MIC values: Out, periplasmic; In, cytoplasmic; and M, membrane. [e] Since production level of the signal-less BlaM fused at its C-terminus with full-length AspT$_{Ct}$ was low, this BlaM-full-length AspT$_{Ct}$ fusion had a low MIC in the presence of carbenicillin.

activity ($<10 \times 10^{-4}$ units/OD$_{650}$) was observed when the fusion sites were located after Leu^{36}, Leu^{44}, Ser^{88}, Arg^{190}, Val^{258}, Lys^{383}, Trp^{428}, Lys^{433}, Leu^{446}, Ala^{453}, Arg^{502}, and Lys^{529} of AspT$_{Ct}$. PhoA-fusion analysis of AspT$_{Ct}$ suggested that AspT$_{Ct}$ had 7 TMs, a periplasmic C-terminus, and a large cytoplasmic loop located between TM4 and TM5. The large cytoplasmic loop was the unique feature of the two-dimensional structure of AspT. But unlike the periplasmic N-terminus of AspT$_{Th}$, the N-terminus of AspT$_{Ct}$ seemed to be located in the cytoplasm (Fig. 2).

Analysis of AspT$_{Ct}$–BlaM Fusion Proteins—To confirm the unique two-dimensional structure of AspT$_{Ct}$ and the structural differences between AspT$_{Ct}$ and AspT$_{Th}$, we examined the implications of the AspT$_{Ct}$–PhoA fusion results by using BlaM–AspT$_{Ct}$ fusions for N-terminal analysis and AspT$_{Ct}$–BlaM fusions for analysing other junction positions with the C-terminus of AspT$_{Ct}$. We designed two BlaM–AspT$_{Ct}$ fusion genes: one encoded β-lactamase lacking its signal sequence and fused at its C-terminus with the full-length of AspT$_{Ct}$, and the other encoded the same protein fused with the N-terminal half of AspT$_{Ct}$. To examine proper expression of the fusion proteins in the *E. coli* hosts, we ran SDS–PAGE of extracts prepared from a membrane fraction of the cells harboring the plasmids, and we visualized the protein by immunoblotting using antibacterial β-lactamase rabbit polyclonal antibodies. The results (Fig. 1, B and C) show that the fusion proteins from Gly^{23} through Ala^{561} lined up according to increasing molecular mass as the fusion sites approached the C-terminal end of the full-length protein. Some fusion proteins yielded extra bands having lower molecular mass than expected, a result that suggests proteolysis. Production of the signal-less BlaM fused at its C-terminus with the N-terminal full-length and half of AspT$_{Ct}$ was observed. AspT$_{Ct}$–BlaM fusion proteins with fusion locations at Gly^{23}, Lys^{61}, Leu^{115}, Glu^{142}, Ser^{422}, Gln^{462}, Thr^{477}, and the C-terminal end Ala^{561} of AspT$_{Ct}$ showed carbenicillin resistance (200–400 μg/ml), suggesting that the fusion sites including C-termini faced the periplasm. On the contrary, signal-less BlaM fused at its C-terminus with the N-terminal full-length and half of AspT$_{Ct}$, and the remaining AspT$_{Ct}$–BlaM fusion proteins with junction sites at Leu^{36}, Leu^{44}, Ser^{88}, Ala^{196}, Val^{258}, Lys^{383}, Trp^{428}, Lys^{433}, Leu^{446}, Ala^{453}, Arg^{502}, and Lys^{529} were sensitive to carbenicillin at concentrations <100 μg/ml, indicating that these fusion sites were most likely located on the cytoplasmic side of the membrane. The fusion proteins with junction sites at Gly^{23} and Ala^{561} that were produced with pYZ showed an MIC of 800 μg/ml for carbenicillin, and those expressed with pET showed an MIC of 400 μg/ml (Table 1).

When BlaM fusions to the N-terminal or the C-terminal of the full length of AspT$_{Ct}$ were induced with IPTG higher than 40 μM, cells producing the fusions were unable to grow on carbenicillin-free LB-plates. The BlaM fusion to the N-terminal half of AspT$_{Ct}$ survived on carbenicillin-free LB agar plates when the fusion was highly induced in pET with 40 μM IPTG. AspT$_{Ct}$–BlaM fusion proteins with fusion locations at Gly^{23}, Ala^{195}, Trp^{428}, and Ala^{453} were also induced in pET with 40 μM IPTG, and the cells producing the fusion constructs were able to grow on carbenicillin-free LB agar plates. Cells producing the BlaM fusion to the N-terminal half of AspT$_{ct}$ induced by 40 μM IPTG on pET plasmids, was not resistant to 25 μg/ml carbenicillin on LB agar plates. All BlaM fusions which were not resistant to 25 μg/ml carbenicillin on LB agar plates under induction conditions with 25 μM IPTG were also not resistant to 25 μg/ml carbenicillin under induction conditions with 40 μM IPTG (data not shown).

The results obtained with BlaM fusions are in agreement with those obtained with AspT$_{Ct}$–PhoA fusion proteins (Table 1). For the following reasons, the results of PhoA- and BlaM-fusion analyses indicated the possibility of two reentrant loops (Phe^{31}–Ile^{49}, Phe^{426}-Val^{456}) that seem to be embedded in the cytoplasmic membrane from the outside between TM1 and TM2 and between TM5 and TM6, respectively. Cells expressing PhoA and BlaM fused with AspT$_{Ct}$ at Gly^{23}, Lys^{61}, Ser^{422}, and Gln^{462} obviously had alkaline phosphatase activity and resistance to carbenicillin, suggesting a periplasmic localization of these sites. However, cells expressing PhoA and BlaM fused at Leu^{36}, Leu^{44}, Trp^{428}, Lys^{433}, and Ala^{453} of AspT$_{Ct}$ showed low levels of alkaline phosphatase activity and resistance to carbenicillin.

The amino acid-chains Gly^{23}–Lys^{61} and Ser^{422}–Gln^{462} are not long enough to traverse the cytoplasmic membrane twice. In addition, if the Leu^{36} and Leu^{44} residues faced the cytoplasm, the putative cytoplasmic loops seemed to lack positive-charged residues that would contribute to retention of the cytoplasmic loops on the cytoplasmic side of membranes, according to the "inside positive rule" (*25, 26*).

The PhoA- and BlaM-fusion analyses of $AspT_{Ct}$ suggest that $AspT_{Ct}$ has 7 TMs, a large cytoplasmic loop containing approximately 200 A.A. residues between TM4 and TM5, a cytoplasmic N-terminus, and a periplasmic C-terminus (Fig. 2). These results suggest that the orientation of the N-terminus of $AspT_{Ct}$ with respect to the cytoplasmic membranes differs from that of $AspT_{Th}$. $AspT_{Th}$ (described in our previous study (*14*)) and $AspT_{Ct}$ (described in this study) are the only transporters for which aspartate:alanine exchange has been biochemically demonstrated. Although the two AspTs carry out the same transport reactions (that is, aspartate:aspartate homologous and aspartate:alanine heterologous antiport reactions), the secondary structures (for example, the orientations of the TMs) of the two AspTs are different. In particular, the N-terminus of $AspT_{Ct}$ appears to face the cytoplasm, whereas that of $AspT_{Th}$ faces the periplasm (*15*).

Major differences between the topologies of the two AspTs were observed in their N-terminal regions (~90 A.A. residues), including TM1. The topologies of other parts (~90 A.A.- C-termini) were relatively similar in having hydrophilic large central loops. However, the amino acid sequences of the large cytoplasmic loops had low levels of similarity. The difference in the distributions of the charged residues in the TMs and the orientations of the TM1s of the two AspTs may reflect differences in their phylogenetic ancestors.

The results of a BLAST [http://www.ncbi.nlm.nih.gov/BLAST/(*27*)] search of nucleotide and protein sequences of these *asp* operons against current nucleotide and protein databases suggest that several Gram-negative bacteria such as *Zymomonas mobilis*, *Ralstonia eutropha*, and *Vibrio alginolyticus* have *asp* operons with gene organization similar to that of the *asp* operon of *C. testosteroni*, and some Gram-positives such as *Lactobacillus acidophilus* possess *asp* operons similar to that of *T. halophilus*. The *aspT* orthologues predicted to be clustered with *aspD* genes are shown in Supplementary Table 1. Moreover, we found 90 *aspT* orthologues, such as *yidE* and *ybjL* of *E. coli*, without forming gene clusters with *aspD* orthologues in 60 bacterial or archial genomes. All of the putative AspT orthologues possess typical conserved aspartate:alanine exchanger Asp-Al_Ex domains listed in the Pfam database (http://www.sanger.ac.uk/cgi-bin/Pfam/getacc?PF06826).

Analyses of hydropathy and sequence alignment of the AspTs suggest that most of the AspT orthologues have 9–11 TMs, with the large hydrophilic loops found in $AspT_{Th}$ and $AspT_{Ct}$. The large hydrophilic loops of the AspT orthologues possess 1 or 2 TrkA_C domains found in the regulatory subunit TrkA of the bacterial potassium:proton symporters TrkH and TrkG (http://www.sanger.ac.uk/Software/Pfam/, accession no. PF06826), as well as in $AspT_{Th}$ and $AspT_{Ct}$. Although the physiological and biochemical functions of the putative AspT orthologues remain uncertain, *aspT* genes are categorized by their gene organization and by whether *aspT* genes form operons with *aspD* genes. Further functional analyses of the remaining AspT orthologues are necessary to increase our understanding of the physiological and phylogenetic characteristics of the AAE family.

We thank Hideki Yukawa (Mitsubishi Chemical Group Science and Technology Research Center) for the gift of the *Comamonas testosteroni* (*P. dacunhae*) strain. We are grateful to Taiji Nakae for the gift of plasmid pBAD*phoA* and *E. coli*. LMG194. Financial support was provided by research fellowships from the Japan Society for Promotion of Science for Young Scientists.

REFERENCES

1. Mardashev, S.R. and Gladkova, V.N. (1948) *Biokhimiya* **13**, 315
2. Meister, A., Sober, H.J., and Tice, S.V. (1951) Determination of aspartic and glutamic acids by enzymatic decarboxylation. *J. Biol. Chem.* **189**, 591–595
3. Nishimura, J.S., Manning, J.M., and Meister, A. (1962) Studies on the mechanism of activation acid beta-decarboxylase by alpha-keto acids and pyridoxal 5′-phosphate. *Biochemistry* **1**, 442–447
4. Cattaneo-Lacombe, J., Senez, J.C., and Beaumont, P. (1958) Purification of 4-aspartic acid decarboxylase of *Desulfovibrio desulfuricans*. *Biochim. Biophys. Acta.* **30**, 458–465
5. Senez, J.C. and Cattaneo-Lacombe, J. (1956) *C. R. Hebd. Seances. Acad. Sci.* **242**, 941–943
6. Crawford, L.V. (1958) Studies on the aspartic decarboxylase of *Nocardia globerula*. *Biochem. J.* **68**, 221–225
7. Cooksey, K.E. and Rainbow, C. (1962) Metabolic patterns in acetic acid bacteria. *J. Gen. Microbiol.* **27**, 135–142
8. Wilson, E.M. (1963) Crystalline L-aspartate 4-carboxy-lyase. *Biochim. Biophys. Acta.* **67**, 345–348
9. Wilson, E.M. and Kornberg, H.L. (1963) Properties of crystalline L-Aspartate 4-carboxy-lase from *Achromobacter* sp. *Biochem. J.* **88**, 578–587
10. Novogrodsky, A. and Meister, A. (1964) Control of Aspartate beta-decarboxylase activity by transamination,. *J. Biol. Chem.* **239**, 879–888
11. Novogrodsky, A., Nishimura, J.S., and Meister, A. (1963) Transamination and beta-decarboxylation of aspartate catalyzed by the same pyridoxal phosphate-enzyme. *J. Biol. Chem.* **238**, 1903–1905
12. Chibata, I., Kakimoto, T., and Kato, J. (1965) Enzymatic production of L-alanine by *Pseudomonas dacunhae*. *Appl. Microbiol.* **13**, 638–645
13. Abe, K., Hayashi, H., and Maloney, P.C. (1996) Exchange of aspartate and alanine. *J. Biol. Chem* **271**, 3079–3084
14. Abe, K., Ohnishi, F., Yagi, K., Nakajima, T., Higuchi, T., Sano, M., Machida, M., Sarker, R.I., and Maloney, P.C. (2002) Plasmid-encoded asp operon confers a proton motive metabolic cycle catalyzed by an aspartate-alanine exchange reaction. *J. Bacteriol.* **184**, 2906–2913
15. Nanatani, K., Ohonishi, F., Yoneyama, H., Nakajima, T., and Abe, K. (2005) Membrane topology of the electrogenic aspartate-alanine antiporter AspT of *Tetragenococcus halophilus*. *Biochem. Biophys. Res. Commun.* **328**, 20–26
16. Shibatani, T., Kakimoto, T., and Chibata, I. (1979) Stimulation of L-aspartate beta-decarboxylase formation by L-glutamate in *Pseudomonas dacunhae* and improved production of L-alanine. *Appl. Environ. Microbiol.* **38**, 359–364

17. Eisenberg, D., Schwarz, E., Komaromy, M., and Wall, R. (1984) Analysis of membrane and surface protein sequences with the hydrophobic moment plot. *J. Mol. Biol.* **179**, 125–142
18. Guan, L., Ehrmann, M., Yoneyama, H., and Nakae, T. (1999) Membrane topology of the xenobiotic-exporting subunit, MexB, of the MexA, B-OprM extrusion pump in *Pseudomonas aeruginosa*. *J. Biol. Chem.* **274**, 10517–10522
19. Schaffner, W. and Weissmann, C. (1973) A rapid, sensitive, and specific method for the determination of protein in dilute solution. *Anal. Biochem.* **56**, 502–514
20. Rozzell, J.D. Method and compositions for the production of L-alanine and derivatives thereof. *U.S. Patent.* 5,019,509.
21. Hirokawa, T., Boon-Chieng, S., and Mitaku, S. (1998) SOSUI: classification and secondary structure prediction system for membrane proteins. *Bioinformatics* **14**, 378–379
22. Krogh, A., Larsson, B., von Heijne, G., and Sonnhammer, E.L. (2001) Predicting transmembrane protein topology with a hidden Markov model: application to complete genomes. *J. Mol. Biol.* **305**, 567–580
23. Sonnhammer, E.L., von Heijne, G., and Krogh, A. (1998) A hidden Markov model for predicting transmembrane helices in protein sequences. *Proc. Int. Conf. Intell. Syst. Mol. Biol.* **6**, 175–182
24. Hofman, K. and Stoffel, W. (1993) TMbase: a database of membrane spanning protein segments. *Biol. Chem. Hoppe-Seyler* **374**, 166
25. von Heijne, G. (1989) Control of topology and mode of assembly of a polytopic membrane protein by positively charged residues. *Nature* **341**, 456–458
26. Andersson, H., Bakker, E., and von Heijne, G. (1992) Different positively charged amino acids have similar effects on the topology of a polytopic transmembrane protein in *Escherichia coli*. *J. Biol. Chem.* **267**, 1491–1495
27. Altschul, S.F., Gish, W., Miller, W., Myers, E.W., and Lipman, D.J. (1990) Basic local alignment search tool. *J. Mol. Biol.* **215**, 403–410